Materials Science Forum Vols. 38-41 (1989) pp 39-50
© (1989) Trans Tech Publications, Switzerland
doi:10.4028/www.scientific.net/MSF.38-41.39

Materials Science Forum Vols. 38-41 (1989) pp. 39-50
Copyright Trans Tech Publications, Switzerland

DEFECT METASTABILITY AND BISTABILITY

G.D. Watkins
Department of Physics, Sherman Fairchild Laboratory 161
Lehigh University, Bethlehem, PA 18015, USA

ABSTRACT

Several important examples of semiconductor defect metastability and bistability of current technological and scientific interest are discussed. In only three of the cases, however, has the microscopic structure of the defect been identified and the mechanism for the phenomena established. These are the interstitial carbon-substitutional carbon pair and interstitial iron-acceptor pairs in silicon, and interstitial hydrogen in the elemental and compound semiconductors. These are treated in some detail for the physical insight they provide to the general problem.

When we consider a defect in what we call "configurational space," i.e., we explore the energy surfaces as we displace the atoms associated with the defect core and its neighbors, we can expect more than one local minimum. Only one of these--the lowest in energy--will be the stable configuration, the one we normally expect to encounter. The others are metastable. However, if the energy barriers and energy differences between the configurations are not excessive, it may still be possible to excite the defect into one or more of its metastable configurations. Its electronic and optical properties will be different for each of the configurations with important consequences to the technological properties of the semiconductor host. As a general rule, this is undesirable. It is important that a device have steady, reproducible properties. On the other hand, controllable metastability could conceivably be useful as a memory device. In any event, it is important to understand the phenomenon and control it. At the same time, the phenomenon presents a challenging scientific puzzle that occupies many of us at this conference today.

I. CONFIGURATIONAL COORDINATE DIAGRAMS

In order to discuss such a system it is convenient to construct a "configurational coordinate" (CC) diagram, where the total energy of the system is plotted vs. a single generalized distortion coordinate Q which serves to describe the combined atomic rearrangements as one passes on a minimum energy path from one local minimum to another in configuration space. In Fig. 1, we

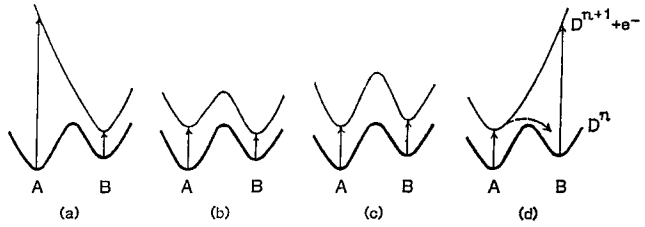

Fig. 1. Four possible CC diagrams for a metastable defect with two lattice configurations.

show a set of such diagrams for a defect which in charge state n has a stable lattice configuration labeled A and a metastable one labeled B, with a barrier between. The four figures differ only in the properties of the excited ionized state $D^{n+1} + e^-$, representing four commonly occurring possibilities. (The ionized state could equally represent $D^{n-1} + h^+$ for excitation to the valence band.) In Figs. 1(a) and (d), the ionized state has a local minimum only in configuration B or A, respectively. These are often referred to as large lattice relaxation (LLR) cases because large Stokes shifts are apparent, the vertical optical ionization energies from one of the configurations being much greater than the true ionization energies. In Figs. 1(b) and (c) the ionized states display both local minima but they differ as to whether A or B is the lowest energy configuration. These in turn are commonly referred to as small lattice relaxation (SLR) cases because large Stokes shifts are absent.

In cases (a) and (b), the stable configuration is different for the D^n and the ionized D^{n+1} charge states. The defect is therefore bistable, and can be converted from one configuration to the other simply by changing its charge state at a temperature at which the barriers can be surmounted. Cooled to below this temperature, the defect is frozen into its respective configuration and its optical and electrical properties can be measured directly. Junction capacitance techniques are therefore ideally suited for the study of these defects because the charge state can be controlled simply by external bias on the junction. All of the relevant photo- and thermal-ionization energies and barriers for conversion can often be extracted from these studies.

For cases (c) and (d), the A configuration remains the stable one for both charge states. Conversion to the B configuration may still be possible, however, by some trick such as optical excitation or electrical injection, denoted symbolically by the dashed line in (d), or as in case (c) by establishing a thermal equilibrium distribution between the two near equal energy configurations in the ionized state, etc.

In what follows, we will consider several specific examples which will serve to illustrate each of the above cases. Unfortunately, for only a very few of these has the identity of the defect and the mechanism for the metastability been reasonably well established. Hopefully the insight that we will gain from these few cases will assist us in unraveling the many other important metastable systems which are not yet identified or understood.

II. HYDROGEN IN SEMICONDUCTORS

The study of hydrogen as an impurity in semiconductors is a hot topic these days because of the important role hydrogen plays in passivating electrically active defects in the materials. Clearly, a first fundamental step in understanding this process is understanding the isolated hydrogen defect in the crystal, how it is incorporated, its electrical properties, how it diffuses through the

lattice, etc.

It is an interesting and surprising fact that until very recently no direct detection of an isolated hydrogen atom has been accomplished in any semiconductor. And yet we know a great deal about it! This information comes from muon spin rotation experiments (μSR) on the light isotope of hydrogen, muonium (μ^o). In these exotic experiments, muons (μ^+) from a polarized beam come to rest capturing an electron in the semiconductor and then decay within their 2.2 μs natural lifetime by emitting a positron preferentially along the nuclear spin axis. In a magnetic field, therefore, the emitted positrons act like a rotating beacon as each muon axis sweeps around the magnetic field at its magnetic resonance precessional frequency. With a positron detector at the side, the oscillations of the positron flux provide a direct measure of the precessional frequency and reveal therefore the same detailed microscopic information available from conventional EPR magnetic resonance spectroscopy. An excellent review article of these experimental techniques and what has been learned using them has very recently been presented by Patterson [1]. The interested reader is referred to this. In what follows we summarize only very briefly the conclusions with primary emphasis on silicon. We include also some important more recent information.

It has been known from these studies for many years now that two distinct configurations exist in basically all elemental and compound semiconductors. One configurations displays full tetrahedral symmetry (T_d) and has been labeled "normal" muonium μ. The other has <111> axial symmetry (C_{3v}) and is labeled "anomalous" muonium μ*. In the elemental semiconductors C, Si, Ge it was further established that μ* is the more stable configuration and is frozen into a specific <111> orientation (at least over the 2.2 μsec lifetime) while μ is highly mobile in the lattice with a diffusion constant estimated as high as $10^{-4}cm^2/sec$ at 20K.

From the outset it was natural to identify μ with a tetrahedral interstitial lattice site (T) but μ* was more difficult. The breakthrough came only two years ago when Cox and Symons suggested that hydrogen would naturally like to assume a position in the center of a <111>-oriented lattice bond [2]. This was subsequently confirmed first by Estle et al. [3] using Hartree-Fock molecular orbital calculations for diamond and by Estreicher [4] for silicon, and shortly thereafter independently by DeLeo et al. [5] and Deak et al [6]. They all find that for neutral muonium there are two local minima, the lowest energy one at the bond center with a second one at (or slightly offset from) the tetrahedral interstitial site. Recently, Van de Walle et al [7]. also concluded that the bond-centered site is the lowest energy configuration using local density pseudopotential theory.

Very recently the bond-centered μ* configuration has been confirmed experimentally by an ingenious direct measurement via μSR of the hyperfine interaction with the two equivalent bonding silicon atoms and their six neighbors [8,9]. (It has also been confirmed by a similar experiment for μ* in GaAs [10].) Very recently, also, direct EPR observation of bond-centered hydrogen has been reported for the first time by Gordeev et al. in proton-implanted silicon at 80K [11]. The direct 1:1 correlation demonstrated by these authors between the spin Hamiltonian parameters of μ* and the hydrogen center appears to make this exciting new identification also unambiguous.

Neutral isolated interstitial hydrogen in silicon therefore supplies us with a very simple example of a metastable defect and one of the very few for which the detailed microscopic configurations appear to have been established. No direct experimental information exists at present, however, concerning its electrical

properties or the configurations appropriate to its ionized states. The recent calculations of Van de Walle et al. [7], however, can serve as a guide. They report having investigated the energy surfaces for H^+, H^o, and H^- and the relative energies of the different charged states. They conclude that for H^+ and H^o the BC site is lowest in energy but that for H^-, the T site is lowest.

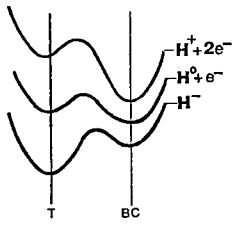

Fig. 2. Schematic CC diagram for H in Si.

In Fig. 2, we sketch a schematic CC diagram which contains a possible consensus of the various theoretical and experimental results [46]. Interestingly, if correct, it provides an example for both cases (b) and (c) of Fig. 2, the $H^- \rightarrow H^o + e^-$ and $H^o \rightarrow H^+ + e^-$ transitions falling respectively into the two different cases. Partial confirmation of this predicted bistability between H^+ and H^- can be deduced from the configurations believed to exist for hydrogen when it passivates acceptors and donors in silicon. The evidence is strong that hydrogen enters the bond-center site when it passivates acceptors (A^-H^+) but is in a displaced back-bonded T site when passivating shallow donors (D^+H^-).

The "small lattice relaxation" (SLR) label for cases (b) and (c) in Fig. 1 is clearly misleading in this case of interstitial hydrogen. The hydrogen moves a distance of the order of a full lattice dimension (2.25 Å) and the silicon neighbors have readjusted ~0.4 Å. In fact, estimates of the relaxation energy stored in the lattice in forming the BC configuration range from 4 eV [7] to 9 eV [6]. This large lattice relaxation has important consequences in understanding the kinetics of the T to BC conversion as well as the various diffusional processes that does not appear to have been previously pointed out. It can be shown, for example, from a simple WKB analysis, that a particle can tunnel through a sinusoidal barrier of height E_B at a rate given approximately by

$$\nu_T \sim \frac{1}{L}\sqrt{\frac{E_B}{2M}}\exp[-4(2ME_B)^{1/2}L/h] \qquad (1)$$

where M is the mass of the particle and L the width of the barrier [12]. This can also serve as a guide for our more complex energy surfaces in CC space if M is taken as the effective mass of the vibrational mode along the Q path (the mass of a quasiparticle) and L the distance between local minima in Q space.

The barrier heights for T to BC conversion as well as the BC to BC and T to T diffusion jumps have been estimated in several recent theoretical papers [4-7]. Although the results differ in detail, the various barrier height estimates range from ~0.2-1.0 eV. Using E_B~0.5 eV and L~2.35 Å as a guide, the muon mass (207 m_e) gives a tunneling frequency of $2.7\times10^{10}\,sec^{-1}$. For the proton mass, the tunneling frequency is greatly reduced but still $2.1\times10^{3}\,sec^{-1}$. This is what might be expected for the diffusional motion from T to T site via the intermediate hexagonal site for which very little silicon relaxation is found. The motion is therefore primarily that of the hydrogen, or muon, with its corresponding atomic mass. On the other hand, for the T to BC conversion and the BC to BC migration the situation is entirely different. Here the large silicon relaxation associated with the motion makes M approach that of the silicon neighbors independent of whether the muon or hydrogen is involved. Now, for a barrier again of 0.5 eV, the tunneling rate is $4\times10^{-41}\,sec^{-1}$, i.e., negligible, and normal thermally activated processes over the barrier are

required.

Therefore even though the various barriers may be comparable, it is the magnitude of the surrounding lattice relaxation that can be the major factor in determining the mobility of the hydrogen in its various configurations. This explains very nicely the fast athermal diffusional mobility observed for normal μ in the T site, but with a thermally activated barrier to the self-trapped BC μ^* state. Our rough estimates above for hydrogen in the T site suggests that we might anticipate similar effects for it.

This leads us to speculate on the mechanism for the curious and apparently different type of acceptor passivation that occurs upon wafer polishing [13]. Is it possible that we are dealing with fast long distance tunneling motion of hydrogen in the T site with passivation then occurring in the metastable back bonding T site? In effect, is the hydrogen metastability manifesting itself also in the B^-H^+ pairs?

In summary, we have learned a remarkable amount of information about hydrogen in silicon without ever having seen it directly. It appears to be a textbook example of meta- and bi-stability, which affects strongly its diffusion and defect pairing processes. There are still many things we would like to know, however, such as its electrical and optical properties. These are difficult to determine in the 2.2 μsec lifetime of muonium. In this context, the recent EPR detection of bond-centered hydrogen is an exciting new development. Now perhaps some of these properties can finally be established.

III. DONOR-ACCEPTOR PAIRS

In many respects, the simplest and most familiar example of metastable configurations is that of donor-acceptor pairs (D^+A^-) in semiconductors. Due to the $-e^2/\epsilon r$ Coulomb interaction between the constituents, the ground state of the neutral pair is at the nearest neighbor separation but there are an unlimited number of excited metastable configurations associated with the discrete more distant lattice separations [14].

When one of the species is a mobile interstitial atom, the barriers for conversion between separations can be low and reversible metastability effects may result. The first clean example of this was in the study of interstitial iron-substitutional aluminum acceptor pairs in silicon [15]. From DLTS studies in p-type material, the detailed CC diagram shown in Fig. 3 could be constructed for the pair. Two hole emission peaks were observed, the deeper one at 0.20 eV being strongly favored when cooled under zero bias (the lower energy curve) and the shallower one at 0.13 eV becoming more prominent when cooled under reverse bias (the upper energy curve). Monitoring the relative intensities of the two peaks vs. T and the kinetics of the conversion from one to the other under the two bias conditions provided all of the relevant energies indicated on the figure.

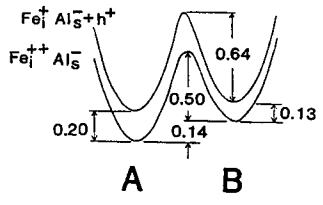

Fig. 3. CC diagram for $Fe_iAl_s^-$ pairs in Si.

An important clue to the identification of the two configurations comes from EPR studies [16] where two distinct $Fe_i^+Al_s^-$ spectra have been observed, one with <111> symmetry indicative of the closest pairs (r=2.35 Å) and the other with C_{2v} <100> symmetry expected for the next nearest pair (r = 2.72 Å). The relative energies of the two

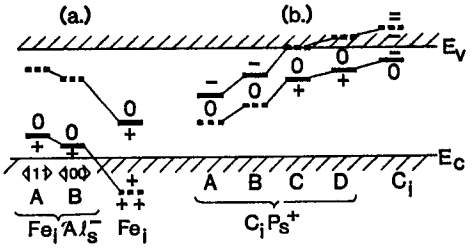

Fig. 4. Electrical levels vs. separation for (a) $Fe_iAl_s^-$ and (b) $C_iP_s^+$ in silicon.

configurations in Fig. 3 matches very closely the predicted Coulomb energy differences for these two separations (ϵ=11.8), completing the identification. In spite of the fact, therefore, that the conversion has not actually been confirmed directly by EPR, the evidence is strong that the two configurations involved have been correctly assigned and that the mechanism is well understood. In Fig. 4(a) we show schematically the origin of the levels, a deeper second donor state (+/++) of iron being lifted out of the valence band by the Coulomb interaction with nearby Al_s^-.

We might anticipate being able to generate and study more distant pairs by DLTS as well for such defects. This apparently is the case for pairs involving interstitial carbon and substitutional donors in silicon. (I say apparently because although a great deal of evidence has been presented for the identification, no direct EPR information exists as yet.) The C_iP_s pair was the first to be discovered [17,18]. Four distinct configurations can be detected by DLTS by first injecting electrically ~240K to create what is probably the most distant pair, and then monitoring vs. anneal as the interstitial carbon atom works its way back in discrete steps to its lowest energy closest-pair configuration. Fig. 4(b) illustrates the evolution of the levels as deduced from these experiments, a second acceptor state of C_i being pulled down from the conduction band by the Coulomb interaction with nearby P_s^+. C_iAs_s and C_iSb_s pairs have also been observed and a detailed description of the C_iSb_s pair studies is being presented at this meeting [19].

IV. EL-2 AND DX

EL-2, a ubiquitous defect in GaAs, and the DX center, a class of defect present in many III-V and II-VI compound semiconductors and their alloys, are currently intensively studied examples of large lattice relaxation metastability. Their presence presents serious technological limitations to the successful device applications of these materials and there is therefore strong motivation to identify and understand them. No overview of metastability would be complete without including them.

1. EL2 in GaAs

EL2 is a dominant deep trap in GaAs [20]. In its stable configuration A it has a DLTS level at E_c-0.75 eV. Optical excitation into an absorption band at 1.15 eV converts the defect into a new configuration B that cannot be detected electrically, optically, or by EPR. The capacitance measured in junction spectroscopy does not change indicating no net change in defect charge state. The thermally activated barrier for return from B→A is ~0.30 eV. The CC diagram that describes this general behavior is case (d) in Fig. 1.

EPR [21] and ODMR [22] studies have provided strong evidence that the As_{Ga} antisite is somehow involved in the core of the defect. Studies of the thermal destruction and regeneration of the defect have led to the suggestion that EL2 is an As_{Ga} antisite-interstitial As_i pair with two distinct configurations [23].

Strong confirmation of this model has been presented by ODENDOR studies for an optical absorption band believed to be associated with the ionized state of the EL2 A configuration [24]. In these studies the presence of an extra nearby As atom in the <111> direction from an As_{Ga} antisite has been detected. Further evidence of C_{3v} <111> symmetry for the stable configuration has been presented in uniaxial stress studies of the photoconversion [25] and anisotropy of phonon scattering from the defect [26].

An alternative model is that it is the isolated As_{Ga} antisite. The most direct experimental evidence of this comes from analysis of uniaxial stress splittings of a zero phonon line at 1.04 eV identified with the photoquenching 1.15 eV transition [27]. This has been interpreted to indicate full T_d symmetry in the A configuration. A strong boost to this "camp" comes from the very recent theoretical conclusions by two independent groups [28,29] that the isolated antisite should display the EL2 behavior, the B configuration resulting from the ejection of the antisite out of its gallium lattice site into the neighboring interstitial site leaving a gallium vacancy behind

$$As_{Ga} \rightarrow As_i + V_{Ga} \qquad (2)$$

And so just when it looked as though EL2 was going to emerge as the $As_{Ga}As_i$ pair, we are not so sure. "Will the real EL2 please stand up?"

2. DX in $Al_xGa_{1-x}As$

I will limit the discussion here to the DX center in $Al_xGa_{1-x}As$, the most intensively studied case. Its general features serve to represent the properties of very similar centers observed in a number of other semiconductor systems (GaAsP, GaSb, InP, CdZnTe, CdF_2, etc.)

From the outset [30] it was recognized that donors were involved, hence the "D." Until rather recently "X" meant that some other defect was also thought to be involved. For $x \geq 0.22$ in the alloy, the characteristic feature is persistent photoconductivity at low temperatures which disappears upon warming the sample. The CC diagram that has been universally applied to explain this is shown in Fig. 5(b) in which the stable neutral configuration B is deep but upon optical excitation the defect converts to configuration A with only a shallow effective-mass-like bound state. Because of the large lattice relaxation involved, a barrier must be overcome to return to the deep state B. This is therefore an example of the bistable case (a) in Fig. 1 (reverse the A and B labels).

For $x \leq 0.22$, A is the stable configuration with the deep B configuration metastable in the conduction band, as shown in Fig. 5(a). In this case it is an example of case (d) in Fig. 1. The presence of this long-lived resonance state in the conduction band can still be demonstrated by filling it with hot carriers [31] or heavy doping [32] or by the application of hydrostatic pressure which serves to push it back into the forbidden gap [33,34].

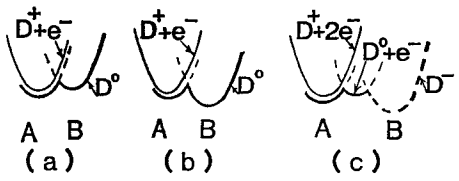

Fig. 5. CC diagrams for DX in $Al_xGa_{1-x}As$. Conventional model for (a) $x \leq 0.22$; (b) $x \geq 0.22$; (c) negative-U model for $x \geq 0.22$.

Over the past very few years, it has become increasingly evident that this is most likely an intrinsic property of the isolated donor itself because the concentration of the DX centers always appears comparable to the total donor concentration. If this is the case, its bistable behavior therefore becomes an example of the shallow-deep instability labeled "extrinsic self-trapping" by Toyozawa [35].

A strong boost to this conclusion comes from very recent calculations by Chadi and Chang [36]. They conclude that donors on the Ga lattice (Si) distort in a manner similar to EL2

$$\underset{(A)}{D_{Ga}} \rightarrow \underset{(B)}{D_i} + V_{Ga} \qquad (3)$$

while for donors on the As lattice (Te), the neighboring Ga atom distorts

$$D_{As} + Ga \rightarrow D_{As} + V_{Ga} + Ga_i \qquad (4)$$

Remarkably they find that the energetics are very nearly the same for the two, consistent with experiment. A surprise of their calculations, however, is that an extra electron must be trapped to stabilize the distorted B configuration. The implied CC diagram is shown in Fig. 5(c) which means that the DX center is a negative-U center, consistent with a recent suggestion by Khatchaturyan, Weber, and Kaminska [37].

The feeling here is that we are getting close to the solution, but we are not quite there.

V. OTHER CENTERS

We mention here briefly three other important examples.

1. The Early Thermal Donors

In silicon containing oxygen, prolonged heat treatment at ~450°C produces a series of double donors called thermal donors. The microscopic structure of the core and the mechanism for formation constitute another hot topic of this conference as has been the case for a number of years. A remarkable relatively recent observation is that the first two in the series are bistable, displaying negative-U properties [38]. Similar results are found in germanium. No microscopic structural model exists as yet.

2. The M-center in InP

The M-center is an irradiation-produced center in InP which displays remarkable bistable properties. In a series of elegant DLTS, TSCAP, and photocapacitance experiments, Stavola et al. [39] have mapped out detailed CC diagrams for it. There are two configurations A and B accessible by cooling under reverse bias or zero bias, respectively. Both reveal large lattice relaxations with substantial Stokes shifts between optical and electrical ionization energies. Configuration A can exist in three different charge states, two of which are in negative-U ordering, and B, in two charge states of normal ordering. Configuration B shows evidence of being comprised further of two similar but distinct configurations B and B'.

The M-center is therefore a most fascinating bistable multielectron trap which displays most all of the interesting properties possible for such a defect. In

terms of the energy surfaces, it is one of our best characterized defects. Unfortunately, we have no clue as to what it is. A center with many similar properties has also been observed in unirradiated Fe-doped InP [40].

3. The C_iC_s Pair in Silicon

I have left this until last for several reasons: (1) The discovery of the bistability of this defect is very recent. (2) Even so, the defect is probably the best understood bistable defect in any solid, the CC diagrams being rather completely mapped out and a detailed microscopic structural identification being established for each of the two configurations. (3) The mechanism for the bistability appears to be somewhat different from the models we have been thinking of in the past.

In Fig. 6, I summarize the properties as recently determined for the interstitial carbon-substitutional carbon pair in silicon [41,42]. The defect is amphoteric producing both an acceptor and a donor level in the gap. Both levels display bistability, the A configuration being the stable one for $(C_iC_s)^-$ and $(C_iC_s)^+$, the B configuration for $(C_iC_s)^o$. The complete CC diagrams determined for the acceptor and donor states are shown in (a) and (b), respectively, of the figure.

The models deduced for the configurations are also shown. In the A-configuration, the defect has a substitutional carbon atom next to a carbon "interstitialcy" in which a carbon-silicon molecule shares a single lattice site, each component being three-fold coordinated. In the B configuration, two substitutional carbon atoms (four-fold coordinated) are in normal lattice sites with a two-fold coordinated interstitial silicon atom squeezed off-center between them. The conversion between the two configurations requires only a simple switching of bonds.

The reason that such detailed information could be obtained for this defect was that DLTS, EPR, photoluminescence (PL), and ODMR could all be successfully applied. In many of the experiments, the kinetics of a particular emission or configuration conversion process could be monitored directly by DLTS, EPR and PL providing unambiguous proof that all three were monitoring the same defect. ODMR studies of the 0.97 eV luminescence provided the key structural information for $(C_iC_s)_B^o$, while EPR was available for $(C_iC_s)_A$, $(C_iC_s)_B^-$ and $(C_iC_s)_A^+$.

The structure of the isolated interstitial carbon atom has previously been established by EPR studies to be a <100>-oriented carbon-silicon molecule on a single lattice site [43]. The A configuration can be easily visualized, therefore, as an electrically inactive substitutional carbon atom located in such a position that due to its smaller size

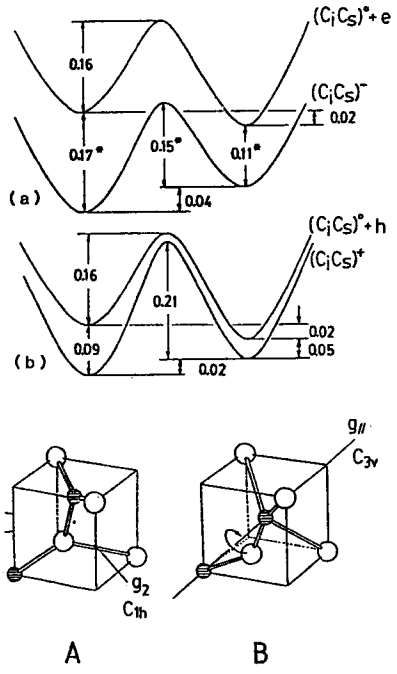

Fig. 6. Models and CC diagrams for the C_iC_s pair in silicon. (a) acceptor state, (b) donor state. The smaller, cross-hatched atoms are carbon.

it optimally reduces the compressional strain of the Si-Si-Si side of the carbon interstitialcy. This suggests that the origin of the binding is primarily strain relief and no long range Coulomb interaction exists. Consistent with this picture, the electrical and EPR properties of the A configuration are observed to be only slightly perturbed from those of the isolated interstitial carbon.

The B configuration, on the other hand, is an interesting rearrangement of the constituents. Viewed as molecular bond switching, there has been no change in the number of saturated bonds or, alternatively, no change in the number of dangling orbitals which supply the electrical activity (one each on the Si and C molecular partners for A, two on the bridging Si for B). Consistent with this we note that the difference in energy between the A and B configurations in any of the charge states is really very small (~.02-.04 eV). The choice as to which is the lower energy configuration vs. charge state is obviously a very subtle effect.

VI. SUMMARY

Defect metastability and/or bistability are turning out to be more and more common occurrences in semiconductors. In only three cases, however, have we really nailed down the identity of the defect and the mechanism for the phenomenon. These are the C_iC_s pair and the Fe_i-acceptor pairs in silicon, and interstitial hydrogen (muonium) in the elemental and compound semiconductors.

The phenomenon is easy to visualize for a pair of defects. Simple Coulomb attraction that is charge state dependent between donor-acceptor pairs provides the mechanism for the Fe-acceptor pairs. Molecular bonding rearrangements when one of the pair is an interstitial provides another mechanism as represented by the C_iC_s pair. Perhaps both mechanisms are operative to explain the complex behavior of M and FeM centers in InP and what are believed to be the C_i-group V donor complexes.

Isolated single atom point defects may also display these effects. An interstitial with more than one lattice configuration is the simplest example, as exemplified by hydrogen or muonium in the tetrahedral semiconductor lattice. "Extrinsic self-trapping" represents another often discussed mechanism. Here a "shallow-deep instability" is visualized as arising from a latent tendency for carrier self-trapping (small polaron formation) in the semiconductor that is made possible by the additional central cell potential of a defect. Often in these cases the lattice relaxation is a symmetry lowering one and can be viewed as a Jahn-Teller distortion of an excited degenerate electronic state of the defect. This is not necessary, however [44].

We know that extrinsic self-trapping occurs. Strong evidence has been presented that this is the mechanism for CdF_2:In [45], which we have treated here as a member of the DX family. The weight of the evidence now swings also toward this interpretation for all of the DX family. And yet it is interesting to note that there has been no direct EPR confirmation or identification in any of these systems. One recently suggested explanation for the failure of EPR is that these centers are really negative-U ones with the paramagnetic state unstable. Still, there are often ways to reveal the paramagnetic states of negative-U centers and we won't really be satisfied until EPR results establish for sure the defect structure and the bistable mechanisms.

Finally, we have TD1 and 2, for which we have no clues as yet, and EL-2, for which we seem to have too many.

This review was made possible by support from the Office of Naval Research Contract No. N00014-84-K-0025. Helpful conversations with G. G. DeLeo concerning hydrogen in silicon are gratefully acknowledged.

REFERENCES

1) Patterson, B.D.: Rev.Mod.Phys., 1988, 60, 69.
2) Cox, S.F.J., and Symons, M.C.R.: Chem.Phys.Lett., 1986, 126, 516.
3) Estle, T.L., Estreicher, S., and Marynick, D.S., Phys.Rev.Lett., 1987, 58, 1547.
4) Estreicher,S., Phys.Rev.B, 1987, 36, 9122.
5) DeLeo, G.G., Dorogi, M.J. and Fowler, W.B.: Phys.Rev.B, 1988, in press.
6) Deák, P., Snyder, L.C. and Corbett, J.W.: Phys.Rev.B, 1988, 37,6887.
7) Van de Walle, C.G., Bar-Yam, Y. and Pantelides, S.T.: Phys.Rev.Lett., 1988,60,2761.
8) Kiefl, R.F., Celio, M., Estle, T.L., Kreitzman, S.R., Luke, G.M., Riseman, T.M., and Ansaldo, E.J.: Phys.Rev.Lett., 1988, 60, 224.
9) Estle, T.L., Kiefl, R.F., Celio, M., Kreitzman, S., Luke, G.M., Riseman, T.M., and Ansaldo, E.J.: B.Am.Phys.Soc., 1988, 33, 699.
10) Kiefl, R.F., Celio, M., Estle, T.L., Luke, G.M., Kreitzman, S.R., Brewer, J.H., Noakes, D.R., Ansaldo, E.J. and Nishiyama, K.: Phys.Rev.Lett., 58 1780 (1987).
11) Gordeev, V.A., Gorelkinskii, Y.V., Konopleva, R.F., Nevinnyi, N.N., Obukhov, Y.V. and Firsov, V.G.: preprint, 1987.
12) Ammerlaan, C.A.J. and Burgemeister, E.A.: Phys.Rev.Lett., 1981, 47,954.
13) Schnegg, A., Grundner, M. and Jacob, H.: in Semiconductor Silicon 1986, ed. by H. R. Huff, T. Abe and B. Kolbesen (Electrochem.Soc. Vol. 86-4, Pennington 1986) p. 198.
14) Dean, P.J.: Prog. in Sol.St.Chem., 1973, 8, 1.
15) Chantre, A. and Bois, D.: Phys.Rev.B., 1985, 31, 7979.
16) Van Kooten, J.J., Weller, G.A. and Ammerlaan, C.A.J.: Phys.Rev.B, 1984, 30, 4564.
17) Song, L.W., Benson, B.W. and Watkins, G.D.: Phys.Rev.B, 1986, 33, 1452.
18) Chantre, A. and Kimerling, L.C.: Appl.Phys.Lett., 1986, 48, 1000.
19) Benson, B.W., Gurer, E. and Watkins, G.D., these proceedings.
20) Martin, G.M. and Markram-Ebeid, S., in Deep Centers in Semiconductors, ed. by S.T. Pantelides (Gordon and Breach, New York 1986), Ch. 6.
21) Weber, E.R. and Omling, Pär: Festkorperprobleme, 1985, XXV, 623.
22) Meyer,B.K., Spaeth,J.M. and Scheffler,M.: Phys.Rev.Lett.,1984,52,851.
23) von Bardeleben, H.J., Stievenard, D., Deresmes, D., Huber, A. and Bourgoin, J.C.: Phys.Rev.B., 1986, 34, 7192.
24) Meyer, B.K., Hoffman, D.M. and Spaeth, J.M.: Mat.Sci.For., 1986, 10-12, 311.
25) Levinson, M. and Kafalas, J.A.: Phys.Rev.B, 1987, 35, 9383.
26) Culbertson, J.C., Strom, U. and Wolf, S.A.: Phys.Rev.B, 1987, 36, 2962.
27) Kaminska,M., Skowronski,M. and Kuszko,W.: Phys.Rev.Lett.,1985,55, 2204.
28) Dabrowski, J. and Scheffler, M.: Phys.Rev.Lett., 1988, 60, 2183.
29) Chadi, D.J., and Chang, K.J.: Phys.Rev.Lett., 1988, 60, 2187.
30) Lang, D. in Deep Centers in Semiconductors, ed. by S.T. Pantelides (Gordon and Breach, New York 1986), Ch. 7.
31) Theis, T.N.: Mat. Sci. For., 1986, 10-12, 393.
32) Theis,T.N., Mooney,P.M. and Wright,S.L.: Phys.Rev.Lett., 1988, 60, 361.
33) Mizuta, M., Tachikawa, M., Kukimoto, H. and Minomura, S.: Jpn.J.Appl.Phys. Pt.2, 1985, 24, L143.
34) Tachikawa, M., Fujisawa, T., Kukimoto, H., Shibata, A., Oomi, G. and Minomura, S.: Jpn.J.Appl.Phys.Pt.2, 1985, 24,L893.
35) Toyozawa, Y.: Physica, 1983, 116B, 7.
36) Chadi, D.J. and Chang, K.J.: to be published.
37) Khachaturyan, K., Weber, E.R. and Kaminska, M.: these proceedings.

38) Makarenko, L.F., Markevich, V.P. and Murin, L.I.: Sov.Phys.Semic., 1985, 19, 1192.
39) Stavola, M., Levinson, M., Benton, J.L. and Kimerling, L.C.: Phys.Rev.B., 1984, 30, 832.
40) Levinson, M., Stavola, M., Besomi, P., and Bonner, W.A.: Phys.Rev.B., 1984, 30, 5817.
41) Song, L.W., Zhan, X.D., Benson, B.W. and Watkins, G.D.: Phys.Rev.Lett., 1988, 60, 460.
42) Song, L.W., Zhan, X.D., Benson, B.W., and Watkins, G.D.: in Defects in Electronic Materials ed. by M. Stavola, S. J. Pearton and G. Davies (MRS Proceedings Vol. 104, Pittsburgh 1988) p. 79.
43) Watkins, G.D. and Brower, K.L.: Phys.Rev.Lett., 1976, 36, 1329.
44) Langer, J.M., Ogonowska, U. and Iller, A., in Physics of Semiconductors 1978 (I.O.P.Conf.Se. 43, Bristol 1979) p. 277.
45) Dmochowski, J.E., Langer, J.M., Kalinski, Z. and Jantsch, W.: Phys.Rev.Lett., 1986, 56, 1735.

46) The calculations of Van de Walle et al [7] predict only one local minimum for each charge state. The secondary minima sketched in Fig. 2 for H^+ and H^- may therefore not exist. We are led to conclude, however, from the muonium results that at least for the neutral state two local minima do indeed exist (μ and μ^*) with a barrier between, as found in all of the earlier theoretical calculations [3-6]. This serves as a caution to not overinterpret the obviously powerful local density results at this early stage in their development.

Defects in Semiconductors 15
10.4028/www.scientific.net/MSF.38-41

Defect Metastability and Bistability
10.4028/www.scientific.net/MSF.38-41.39